ORIGINAL ARTICLE

Novel Molecular and Phenotypic Insights into Congenital Lung Malformations

Daniel T. Swarr[1]*, William H. Peranteau[2]*, Jennifer Pogoriler[3], David B. Frank[4,5,6], N. Scott Adzick[2], Holly L. Hedrick[2], Mike Morley[6], Su Zhou[6], and Edward E. Morrisey[6,7]

[1]Division of Neonatology and Pulmonary Biology, Cincinnati Children's Hospital Medical Center, Cincinnati, Ohio; [2]Department of Surgery, [3]Department of Pathology, and [4]Division of Pediatric Cardiology, Department of Pediatrics, Children's Hospital of Philadelphia, Philadelphia, Pennsylvania; and [5]Department of Pediatrics, [6]Penn Center for Pulmonary Biology, and [7]Department of Medicine, University of Pennsylvania School of Medicine, Philadelphia, Pennsylvania

ORCID ID: 0000-0002-7305-0442 (D.T.S.).

Abstract

Rationale: Disruption of normal pulmonary development is a leading cause of morbidity and mortality in infants. Congenital lung malformations are a unique model to study the molecular pathogenesis of isolated structural birth defects, as they are often surgically resected.

Objectives: To provide insight into the molecular pathogenesis of congenital lung malformations through analysis of cell-type and gene expression changes in these lesions.

Methods: Clinical data, and lung tissue for DNA, RNA, and histology, were obtained from 58 infants undergoing surgical resection of a congenital lung lesion. Transcriptome-wide gene expression analysis was performed on paired affected and unaffected samples from a subset of infants ($n = 14$). A three-dimensional organoid culture model was used to assess isolated congenital lung malformation epithelium ($n = 3$).

Measurements and Main Results: Congenital lung lesions express higher levels of airway epithelial related genes, and dysregulated expression of genes related to the Ras and PI3K–AKT–mTOR (phosphatidylinositol 3-kinase–AKT–mammalian target of rapamycin) signaling pathways. Immunofluorescence confirmed differentiated airway epithelial cell types throughout all major subtypes of congenital lung lesions, and three-dimensional cell culture demonstrated a cell-autonomous defect in the epithelium of these lesions.

Conclusions: This study provides the first comprehensive analysis of the congenital lung malformation transcriptome and suggests that disruptions in Ras or PI3K–AKT–mTOR signaling may contribute to the pathology through an epithelial cell-autonomous defect.

Keywords: congenital cystic adenomatoid malformation of the lung; congenital pulmonary airway malformation; structural birth defects; branching morphogenesis; lung development

Congenital lung lesions are a developmental abnormality of the lung leading to a focal mass of malformed lung tissue. Lesions typically occur sporadically, do not recur in families, and are uncommonly associated with other structural birth defects in modern cohorts (1–3). The incidence of congenital lung malformations is estimated at 1 in 11,000–35,000 live births, comparable to other major malformations such as congenital diaphragmatic hernia (4–6). In the United States, surgical removal of the affected lung lobe in symptomatic and asymptomatic infants is standard clinical practice, due to risk of recurrent pneumonia and theoretical concern for malignant transformation (7, 8). Routine access to affected and "unaffected" lung tissue from each patient makes congenital lung lesions a unique and tractable model to study the

(Received in original form June 24, 2017; accepted in final form January 9, 2018)

*These authors contributed equally to this work.

Supported by NIH grants 4K12HD043245 (D.T.S.), 7K08HL130666 (D.T.S.), and 4R01HL087825 (E.E.M.); a Thrasher Early Career Award (D.T.S.); and a Parker B. Francis Fellowship Award (D.T.S.).

Author Contributions: Performed experiments: D.T.S., W.H.P., J.P., S.Z., and D.B.F. Designed the studies: D.T.S., W.H.P., E.E.M., and D.B.F. Analyzed the data: D.T.S., W.H.P., N.S.A., H.L.H., J.P., D.B.F., M.M., and E.E.M. Wrote the manuscript: D.T.S., W.H.P., J.P., and E.E.M.

Correspondence and requests for reprints should be addressed to Edward E. Morrisey, Ph.D., Translational Research Center, 11th Floor, Room 179, 3400 Civic Center Boulevard, Building 421, Philadelphia, PA 19104-5159. E-mail: emorrise@mail.med.upenn.edu.

This article has an online supplement, which is accessible from this issue's table of contents at www.atsjournals.org.

Am J Respir Crit Care Med Vol 197, Iss 10, pp 1328–1339, May 15, 2018

Originally Published in Press as DOI: 10.1164/rccm.201706-1243OC on January 12, 2018
Internet address: www.atsjournals.org

At a Glance Commentary

Scientific Knowledge on the Subject: Congenital lung malformations are isolated structural birth defects characterized by focal disruption of normal lung development. These lesions are thought to originate from the airway tree as a result of a disruption in branching morphogenesis, but their etiology and pathogenesis remain unknown.

What This Study Adds to the Field: This study integrates clinical, histological, and transcriptome-wide gene expression data, as well as three-dimensional organoid modeling, from a prospective cohort of 58 infants with congenital lung malformations. These data demonstrate that congenital lung lesions consist of differentiated airway structures that are transcriptionally characterized by increased expression of airway epithelial markers and demonstrate dysregulated expression of genes related to the Ras and PI3K–AKT–mTOR (phosphatidylinositol 3-kinase–AKT–mammalian target of rapamycin) signaling pathways. *Ex vivo* disease modeling using three-dimensional organoids demonstrates that there is a cell-autonomous defect in growth and differentiation of the lung epithelium. This study provides the first transcriptome-wide characterization of the gene expression changes that occur in congenital lung lesions. The data support an epithelial intrinsic role in the pathogenesis of congenital lung lesions and provide insight into the molecular pathways underlying this poorly understood group of disorders.

pathogenesis of isolated structural birth defects.

The etiology and molecular pathogenesis of congenital lung lesions remain unknown (9–11). Congenital lung malformations include bronchogenic cysts, congenital pulmonary airway malformations (CPAMs), intralobar sequestrations, extralobar sequestrations, and congenital lobar emphysema. Although originally described as distinct entities, considerable overlap exists in how these lesions are defined. The Stocker classification for congenital lung lesions is based on histology and the presumed site of origin during lung development, with type 0 speculatively originating from the tracheobronchial tree, through type 4, the latter thought to arise from distal alveolar regions (2, 3). Clinically, lesions are commonly grouped by cyst size (microcystic vs. macrocystic) and origin of vascular supply (i.e., presence of an anomalous systemic arterial vessel, and pulmonary vs. systemic venous drainage) (12).

Despite many anatomical and histologic classifications of congenital lung malformations, detailed molecular characterization is lacking. Previous reports have demonstrated that increased expression of FGF7 (fibroblast growth factor 7) or FGF10 in rodent models produces lung malformations resembling CPAMs (13–16). Although clinical studies have failed to show alterations in FGF10 expression levels in human CPAMs, laser microdissection of CPAM epithelium demonstrated increased expression of FGF9 (17, 18). Other studies have suggested that altered expression of vascular endothelial growth factor receptor 2 or α_2-, α_3-, and β_1-integrins or E-cadherin may also contribute to the pathogenesis of CPAMs (19, 20). Somatic mutations in *KRAS* at codon 12 (G12D) have also been identified in CPAMs (21).

In the present study, we employ a combination of transcriptome analysis, histologic assessment of affected tissues, and disease modeling using a three-dimensional organoid culture system to explore the molecular pathogenesis of congenital lung malformations. Our data implicate a primary epithelial cell-autonomous defect that disrupts normal branching morphogenesis. Dysregulated Ras signaling or PI3K–AKT–mTOR (phosphatidylinositol 3-kinase–AKT–mammalian target of rapamycin) signaling is observed and may play a role in the pathogenesis of this disorder. These data provide important insights into the pathogenesis of congenital lung lesions, and demonstrate that CPAMs provide a unique model system to study the etiology of structural birth defects and other pediatric lung disorders.

Methods

Study Design, Subjects, and Lesion Type Definitions

Fifty-eight subjects presenting for surgical resection of a congenital lung lesion between birth and 1 year of age at the Children's Hospital of Philadelphia were enrolled from May 15, 2013, to August 5, 2016, in the institutional review board–approved registry-biorepository, "Clinical and Molecular Characterization of Isolated and Syndromic Anomalies of the Foregut" (Children's Hospital of Philadelphia IRB 12-009788). We assigned each lesion a clinical classification based on prenatal and postnatal imaging, the surgeon's findings at the time of resection, and pathologic findings using the definitions listed in Table E1 in the online supplement. Microcystic and macrocystic CPAMs, intralobar bronchopulmonary sequestration (BPS) lesions, and hybrid lesions were all included. Congenital lobar emphysema, bronchogenic cysts, and cystic lung lesions suspected to be of an acquired etiology (e.g., bronchopulmonary dysplasia, infection) were excluded. Because atretic bronchial segments have been observed in most lesion types when carefully microdissected, we chose to exclude "bronchial atresia" as a distinct diagnostic category for this study (22, 23). A comprehensive set of prenatal and postnatal data was collected for each subject. Tissue samples from the lung lesion, and when available adjacent unaffected tissue from the resected lung lobe, were obtained directly from the operating room. Each sample was cut into three pieces—one piece was placed into 10% formalin for histology, another in cell lysis solution (5 Prime) for DNA isolation, and the third piece in RNA*later* (Thermo Fisher Scientific) for RNA isolation. *See* the online supplement for a complete description of sample biobanking methods.

Histology, Immunofluorescence, and Gene Expression Studies

Paraffin embedding of tissues, standard staining (hematoxylin and eosin [H&E], Alcian blue, Weigert's elastin stain), and immunofluorescence microscopy were performed as described previously (24). For gene expression studies, biotinylated cRNA probe libraries were generated from total lung RNA samples and used with Affymetrix human gene 2.0 ST arrays.

Microarray data were analyzed with the Oligo package available at the Bioconductor website (http://www.bioconductor.org). *See* the online supplement for a complete description of methods and antibodies used. The Gene Expression Omnibus accession number for the microarray data is GSE100442.

Three-Dimensional Organoid Cell Culture Modeling

Lung organoids were generated as described previously, using lung epithelium isolated from the CPAM lesion itself or adjacent healthy lung tissue by flow cytometry (25). *See* the online supplement for a complete description of methods and antibodies used.

Results

Macrocystic CPAMs Are Associated with an Increased Incidence of Neonatal Respiratory Failure and Need for Early Surgical Resection

A total of 58 lesions were obtained from 58 patients. The majority of infants were born at term (median gestation age, 39 wk; range, 31 wk and 4 d to 42 wk gestation), with birthweights appropriate for gestational age (median, 3,305 g; range, 1,300–4,763 g). No significant differences were observed between lesion types. There was a slight male predominance (41 of 58 subjects; 71%). CPAMs were the most common lesion identified (34 of 58 subjects; 59%), with microcystic lesions occurring at more than twice the frequency of macrocystic lesions (74% vs. 26% of CPAMs) (Table 1). Hybrid lesions were the second most common lesion type (22 of 58; 38%). Only two sequestrations (3.4%) were identified that did not appear to have any significant CPAM elements on histopathologic analysis. Twenty-six percent (15 of 58) of patients had respiratory failure after birth directly attributable to the lung lesion and required mechanical ventilation. Infants with macrocystic lung lesions were significantly more likely to have respiratory failure at birth (odds ratio, 15.6; 95% confidence interval, 2.8–87.7; $P = 0.002$), even after removing infants with potentially confounding factors such as prematurity (odds ratio, 8.9; 95% confidence interval, 1.9–42.4; $P = 0.0062$). Similarly, infants with macrocystic lesions were significantly more likely to require early surgical resection compared with all other lesion types (median age at resection, 0 d; range, 0–66 vs. 55 d; range, 0–325 d; Mann-Whitney U score, 73.5; $Z = 3.15$; $P = 0.0016$) (*see* Table 1). Our finding of an increased incidence of microcystic CPAMs stands in contrast to historical studies documenting a higher prevalence of macrocystic lesions. Patients in those studies were largely identified on the basis of symptomatic presentation or at autopsy. However, our findings are consistent with more recent cohorts in which small, asymptomatic lesions are discovered in the era of routine prenatal diagnosis (26, 27), and suggest that microcystic lesions are the most common lesion type but are frequently asymptomatic, whereas macrocystic lesions are found more commonly in symptomatic infants.

Analysis of the Congenital Lung Lesion Transcriptome

To systematically characterize the gene expression changes occurring within congenital lung malformations, Affymetrix human gene 2.0 ST arrays were performed

Table 1. Patient Characteristics

	Microcystic	Macrocystic	Hybrid	BPS	All Lesions
Number	25	9	22	2	58
Male sex	20 (80%)	6 (67%)	14 (64%)	1 (50%)	41 (71%)
Birthweight*	3,529 (1,300–4,763)	3,289 (2,175–4,255)	3,260 (1,860–4,678)	3,419 (3,160–3,677)	3,305 (1,300–4,763)
Gestational age†	39	38 wk and 2 d	39	38 wk and 4 d	39
Resection age‡	55 (0–302)	0 (0–66)	51.5 (0–121)	209 (93–325)	53 (0–325)
Need for mechanical ventilation, all	7 of 25 (28%)	7 of 9 (78%)	5 of 22 (23%)	0 of 2 (0%)	19 of 58 (33%)
Need for mechanical ventilation, attributable to lesion§	4 of 25 (16%)	6 of 9 (67%)	5 of 22 (23%)	0 of 2 (0%)	15 of 58 (26%)
Other malformations/ syndromes	$n = 6$ (2 with pulmonary hypoplasia/pulmonary HTN; 1 with aortic coarctation; 1 with multiple VSDs/PDA; 1 with congenital hyperinsulinism due to KCNJ11 mutation; 1 with van den Ende–Gupta syndrome)	$n = 4$ (3 with pulmonary hypoplasia/pulmonary HTN, of which 1 infant also had rib hypoplasia; 1 with multifocal atrial tachycardia)	$n = 1$ (apical muscular VSD and PDA)	None	11 of 58 (19%)

Definition of abbreviations: BPS = bronchopulmonary sequestration; HTN = hypertension; PDA = patent ductus arteriosus; RDS = respiratory distress syndrome; VSD = ventricular septal defect.
*Birthweight is reported in grams: median (range).
†Gestational age is reported in weeks (or weeks and days where noted): median.
‡Resection age is reported in days: median (range).
§Patients with a medical indication other than a lung lesion were excluded from this row (microcystic: 2 with prematurity/RDS; 1 with van den Ende–Gupta syndrome; macrocystic: 1 with prematurity/RDS).

on 28 paired samples obtained from 14 patients (6 microcystic, 5 hybrid, 1 BPS, and 2 macrocystic lesions). Principal component analysis demonstrated that microcystic and hybrid/BPS lesions clustered together, separating from the paired unaffected lung along both the first and second principal components. Although analysis of the macrocystic CPAM transcriptome was limited by sample size, these lesions appear to cluster separately from both the healthy lung as well as the microcystic and hybrid/BPS lesions (Figure 1A). On the basis of these findings, microcystic and hybrid/BPS lesions were analyzed together, and were compared with paired unaffected lung tissue (Figures 1B–1F and Tables E3–E12). This comparison revealed 351 unique differentially expressed genes (false discovery rate, <5%) (Table E3). Consistent with the well-established observation that congenital lung lesion cysts are lined by bronchial or bronchiolar epithelium (2, 3, 11), upregulated transcripts were highly enriched for genes known to be expressed in the normal airway epithelium including genes specific for ciliated epithelium (Figure 1E and Tables E6–E8). Gene set enrichment analysis (GSEA) revealed significant enrichment for genes within the Ras, PI3K–AKT–mTOR, and mTOR complex signaling pathways, and transcriptional targets of Myc among the downregulated transcripts. Upregulated transcripts were enriched for genes involved in "chromatin

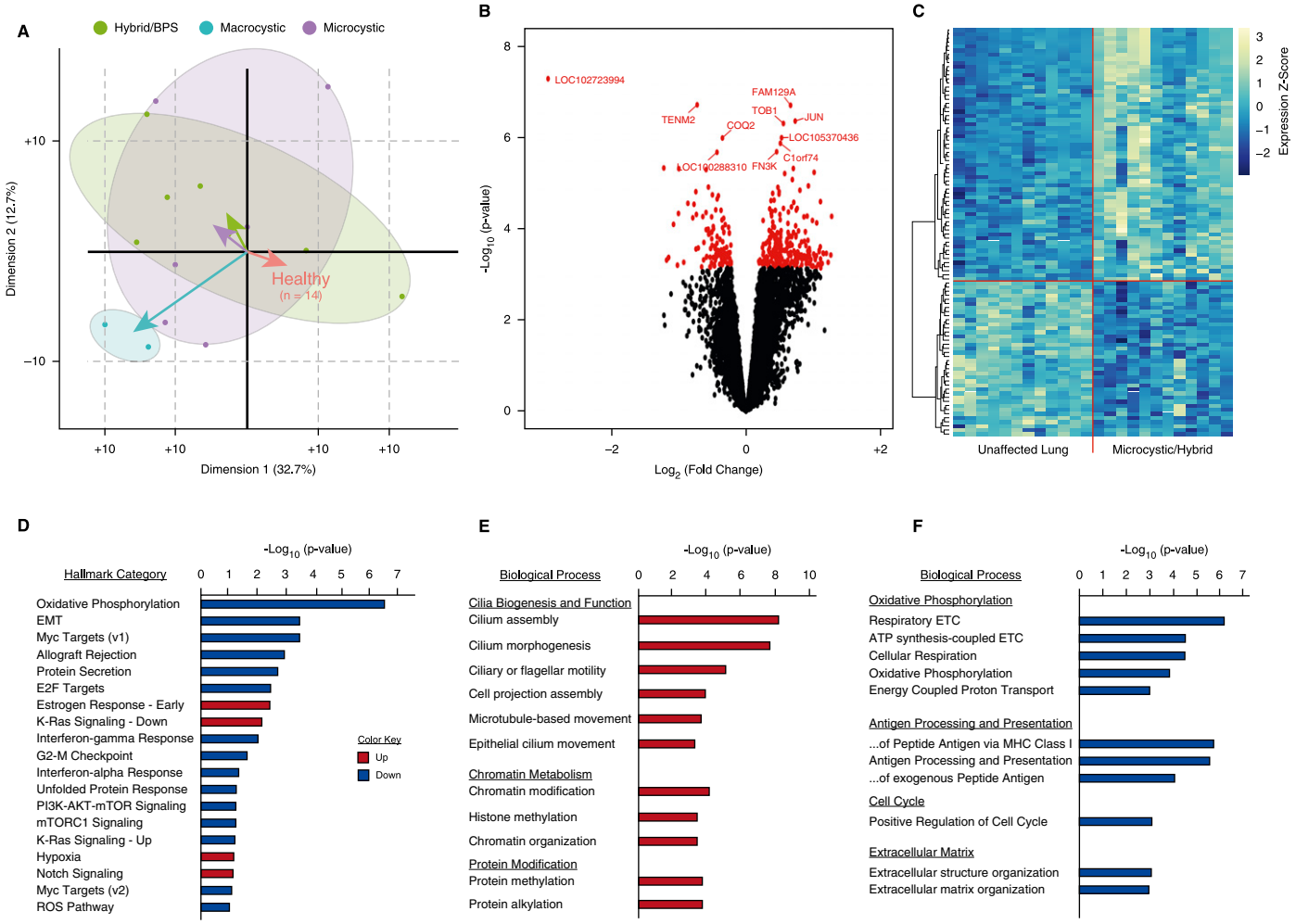

Figure 1. The congenital lung lesion transcriptome. (*A*) A biplot of principal component analysis of gene expression data from 28 paired samples (from 14 patients: 6 microcystic, 5 hybrid, 1 bronchopulmonary sequestration [BPS], and 2 macrocystic lesions) demonstrates that microcystic and hybrid/BPS lesions cluster together, separate from macrocystic lesions, and from paired unaffected lung. Comparison of microcystic/hybrid/BPS lesions with paired healthy lung was used for subsequent analyses. (*B*) Three hundred and fifty-one genes were differentially expressed (false discovery rate, <5%) between microcystic and hybrid lesions compared with paired control lung. (*C*) Unbiased hierarchal clustering based on the top 100 differentially expressed genes demonstrated clear separation of the microcystic congenital pulmonary airway malformation and hybrid/BPS lesion samples from paired normal tissue. Scale to right of heat map illustrates *z*-score color range. (*D*) Gene-set enrichment analysis of differentially expressed genes between microcystic/hybrid/BPS lesions and paired unaffected lung. (*E* and *F*) Gene ontology analysis of differentially expressed genes demonstrates increased expression of genes related to airway epithelium and chromatin/histone modifications, and dysregulated expression of genes related to *KRAS* and PI3K–AKT–mTOR (phosphatidylinositol 3-kinase–AKT–mammalian target of rapamycin) signaling, and Myc transcriptional targets. EMT = epithelial–mesenchymal transition; ETC = electron transport chain; MHC = major histocompatibility complex; mTORC1 = mTOR complex 1; ROS = reactive oxygen species.

modification," "histone methylation," and "chromatin organization," and predicted upstream pathway analysis identified enrichment for targets of the histone methyltransferase KMT2A, and the polycomb proteins ASXL1 and ASXL2 (Figures 1D–1F and Tables E4–E12).

Disrupted Airway Morphology Is a Hallmark of All Congenital Lung Lesions

Standard H&E staining of histological sections collected for research, as well as larger clinical block samples, was reviewed by a pediatric pathologist (J.P.) for all patients enrolled. Immunohistochemical staining was also performed. Cystic structures within congenital lung lesions of all types resemble well-differentiated airway structures, with a ciliated epithelial lining surrounded by smooth muscle (Figures 2 and 3). Epithelial cells lining the lesion express the airway epithelial markers SOX2 and KRT8 (Figure 2). Notable variation in epithelial morphology both within and between lesions and across lesion types was observed, ranging from simple cuboidal to complex pseudostratified epithelia (Figures 2A–2T and E1). Regions of pseudostratified, tall columnar, and simple cuboidal epithelium were observed in lesions clinically classified as macrocystic, microcystic, or hybrid lesions (Figure E1). However, certain histopathologic features seemed to be more characteristic of macrocystic CPAM lesions, including frequent abrupt transitions in the larger cysts between relatively thick walls and alveolar-like sacs, minute papillary

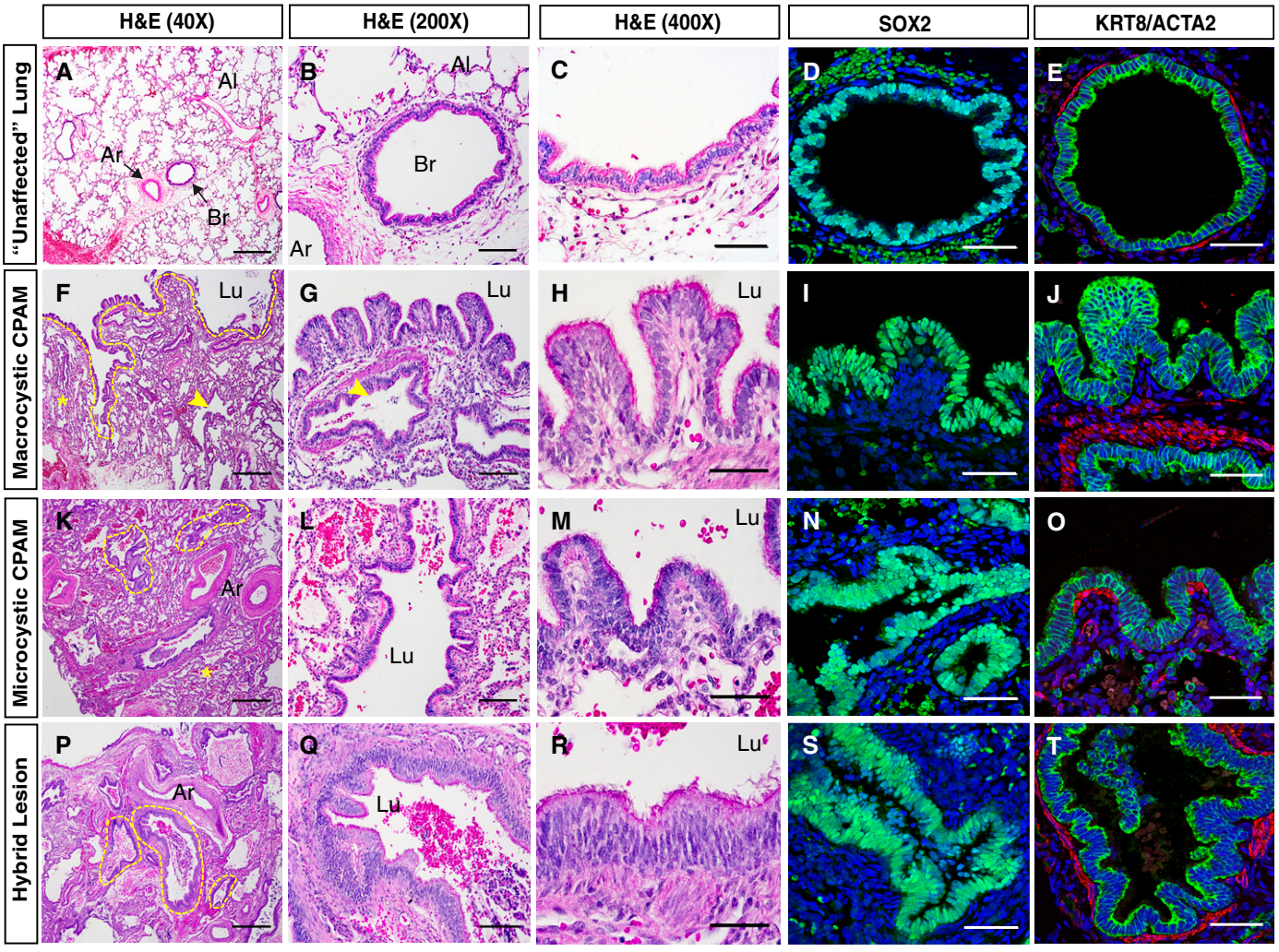

Figure 2. Congenital lung lesion cysts resemble disordered airway structures. (*A–C*) Histological analysis of unaffected lung tissue. (*D* and *E*) SOX2 and KRT8 (green)/ACTA2 (red) expression in unaffected lung tissue, demonstrating a normal bronchovascular bundle surrounded by alveolar tissue. (*F–H*, *K–M*, and *P–R*) Histological analysis of macrocystic (*F–H*), microcystic (*K–M*), and hybrid lesion (*P–R*) tissue. (*I*, *J*, *N*, *O*, *S*, and *T*) SOX2 and KRT8 (green)/ACTA2 (red) expression in macrocystic (*I* and *J*), microcystic (*N* and *O*), and hybrid lesion (*S* and *T*) tissue. A large cystic structure (lumen outlined by dashed yellow line in *F*) is evident in a macrocystic congenital pulmonary airway malformation lesion, which is lined by papillary epithelial structures varying in thickness from columnar to pseudostratified (*F–J*). Smaller cysts (indicated by yellow arrowheads) and compressed alveolar tissue (indicated by yellow asterisks) are also evident. Smaller cysts are highlighted with dashed yellow lines in *K* and *P*. ACTA2 = smooth muscle α-actin; Ar = artery; Al = alveolar region; Br = bronchiole; CPAM = congenital pulmonary airway malformation; H&E = hematoxylin and eosin; KRT8 = keratin, type II cytoskeletal 8; Lu = lumen; SOX2 = SRY (sex-determining region Y)-related HMG box protein 2. Scale bars: (*A*, *F*, *K*, and *P*) 500 μm; (*B*, *G*, *L*, and *Q*) 100 μm; all others, 50 μm.

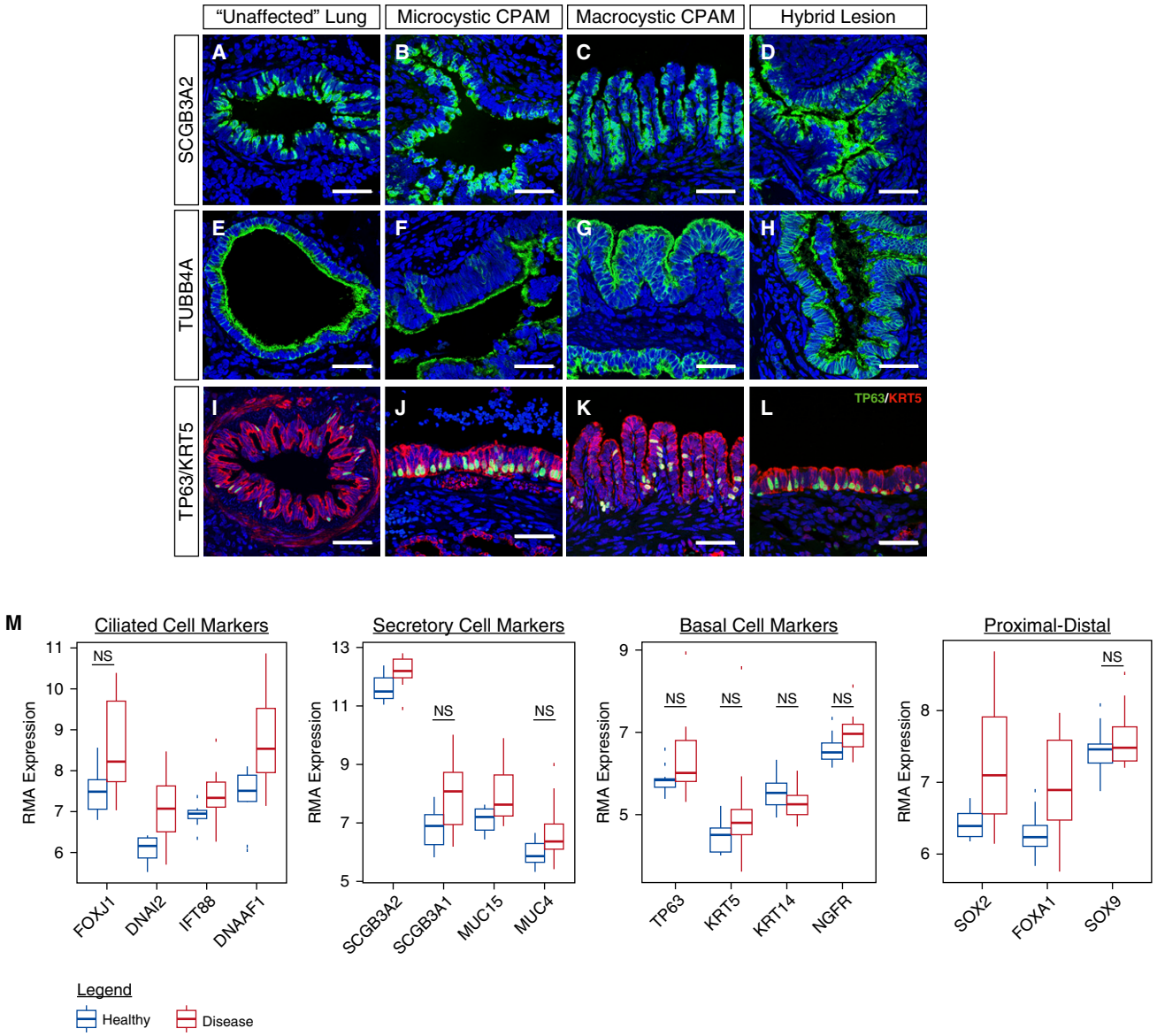

Figure 3. Congenital lung lesion cysts are lined by differentiated airway epithelium. (*A–L*) The epithelial lining of all types of congenital lung lesions was noted to express mature secretory (SCGB3A2), ciliated (TUBB4A), and basal cell (TP63 [green]/KRT5 [red]) markers. (*M*) Significantly increased expression of numerous genes in the airway epithelium was observed by gene expression arrays. Comparison testing was performed with the software package limma, based on a false discovery rate less than 5% accounting for multiple comparisons. Comparisons were significant using these criteria, except where noted. CPAM = congenital pulmonary airway malformation; KRT5 = keratin, type II cytoskeletal 5; NS = not significant; RMA = robust multiarray average; SCGB3A2 = secretoglobin 3A2; TP63 = tumor protein 63; TUBB4A = tubulin, β_4A class. *N* = 12 patients. Scale bars, 50 μm.

projections, and goblet cell metaplasia (Figures 2F–2J, 3C, 3G, 3K, and E2). Goblet cell metaplasia was observed in six of nine macrocystic lesions (67%), ranging from a small cluster of cells to extensive areas of goblet cell hyperplasia resembling mucinous adenocarcinoma *in situ* (Figures E2A–E2E). Only a subset of these macrocystic lesions contained goblet cells where *KRAS* G12D mutations could be identified, consistent with previous reports (Figures E2A–E2E) (21). Of note, only two lesions clinically classified as microcystic based on cyst size (2 of 25; 8%) had areas of goblet cell metaplasia. However, these lesions had other histopathologic features more commonly associated with macrocystic lesions (papillary projections and abrupt transitions). These two lesions illustrate that dominant cyst size measured by radiologic studies may not always correlate with histopathologic descriptions of "microcystic" and "macrocystic" CPAMs.

Immunohistochemistry for the airway secretory cell marker SCGB3A2 and ciliated epithelial cell marker TUBB4A demonstrated that the epithelial lining of CPAM cysts consisted of differentiated airway epithelium (Figures 3A–3D and 3E–3H). Basal cells, indicated by the markers TP63 and KRT5, were frequently found within the cysts and varied in frequency within and between lesions from completely absent to forming a nearly confluent layer (Figures 3I–L and E1). The

distal lung tissue in between these cystic lesions frequently appeared immature, with relatively large and simplified alveoli, decreased numbers of secondary crests, and thickened interstitial spaces. However, these cells expressed distal epithelial markers such as SOX9, SFTPC (type II cell marker), and HOPX (type I cell marker) in the expected patterns, and both protein and gene expression analyses did not reveal significant differences in the ratios of distal alveolar cell types (Figure E3) (28). Taken together, these data support the concept that congenital lung lesions of all types contain tissue in which there is expansion of differentiated airway structures, with impaired development and physical compression of the intervening distal lung.

Abnormal Arterial Vascular Development in a Subset of Congenital Lung Lesions

Both BPS and hybrid lesions, in part defined by the presence of an aberrant arterial blood supply from the systemic circulation, contain hypertrophied and tortuous arterial vessels throughout the lesions (BPS, 2 of 2, 100%; hybrid, 15 of 22, 68%) (Figure 4). However, these vascular abnormalities were not limited to hybrid lesions, and were also seen in two of nine (22%) macrocystic CPAM lesions noted to have a pulmonary arterial blood supply with no identifiable systemic feeding vessel either by presurgical radiologic studies (prenatal ultrasound and/or CT angiography of the chest) or dissection at the time of surgical resection (Figure 4M). Similar changes were not noted in any of the 25 microcystic CPAM lesions (Figure 4M). Abnormal vessels contained normal-appearing arterial endothelium, variable degrees of vascular smooth muscle investment ($TAGLN^+$ cells), and a marked expansion of the vascular adventitial layer consisting of a sparse population of VIM^+ mesenchymal cells invested in a thick layer of extracellular matrix (Figures 4C, 4D, 4G, 4H, 4K, and 4L). These data suggest that expansion of airway structures is associated with abnormal proximal arterial vascular development and/or remodeling.

Three-Dimensional Organoid Modeling Demonstrates a Cell-Autonomous Defect in the Epithelium of Congenital Lung Lesions

To further test the hypothesis that congenital lung lesions result from an as yet undefined cell-autonomous defect in the lung epithelium during development, epithelial cell adhesion molecule (EpCAM; $CD326)^+/CD31^-/CD45^-$ epithelial cells were isolated from CPAM tissue and unaffected adjacent lung by flow cytometric sorting ($n = 3$ patients), and cultured in a three-dimensional organoid model system with an established human lung fibroblast cell line (MRC5) (Figure 5A). After 14 days in culture, the CPAM epithelium consistently formed larger organoids, as revealed by measurement of cross-sectional area (Figures 5B–5D). These large organoids demonstrated a complex stratified epithelium and nearly occlusive lumen, surrounded by at least two or three layers of $TP63^+/KRT5^+$ basal cells, in contrast to the thin single-cell-thick organoids that resemble previously reported tracheospheres in the unaffected epithelial cultures (Figures 5E–5N) (29). Staining for differentiated airway markers, such as SCGB1A1 or TUBB4A, was not observed in either set of cultures. Taken together, these data suggest that CPAM lesions exhibit an epithelial intrinsic defect leading to a disordered growth phenotype consisting of proximal airway structures.

Discussion

Congenital lung lesions have been recognized clinically for more than a century, but the etiology and pathogenesis of this group of disorders have remained unclear (9, 11, 30). A complex array of classification systems and terminologies has evolved to describe congenital lung malformations, yet whether microcystic and macrocystic CPAMs, sequestrations, or hybrid lesions are related to one another at cellular and molecular levels is unknown. Our data suggest that in contrast to the existing literature, microcystic CPAMs are the most common type of congenital lung lesion but are frequently asymptomatic. In contrast, macrocystic CPAMs, although less common, are more likely to be associated with respiratory failure requiring mechanical ventilation and need for surgical resection during the neonatal period. Although it is possible that the lesion type distribution in this study may be impacted by referral bias, our observation that microcystic CPAM lesions is the most common type in the era of prenatal diagnosis is consistent with a larger retrospective review conducted at our own center, as well as other reported patient cohorts (27, 31). We also have observed a relatively low incidence of associated congenital anomalies, compared with older studies. Importantly, before routine use of prenatal ultrasound, lesions were identified only in infants with respiratory distress or infants who died and autopsy was performed, biasing these historical cohorts toward larger, macrocystic lesions or lesions co-occurring with other life-threatening congenital anomalies.

In all lesion types examined, the histology and gene expression data in the current study are consistent with previous observations that congenital lung lesions are dominated by relatively mature airway structures of varying morphology (2, 3). We also observed substantial heterogeneity in histologic findings both within and across lesion types, and even within individual lesions. In the human lung, basal cells and airway smooth muscle extend far down the airway tree, making a precise comparison of congenital lung lesion epithelium to an equivalent position along the proximal–distal axis of the airway tree difficult. However, our data reveal regions of epithelium varying in morphology from simple cuboidal to pseudostratified in all lesion types. Moreover, although abnormal vascular development was nearly a universal feature in BPS lesions, significant proximal arterial vascular abnormalities, including vessel tortuosity, variable expansion of the vascular smooth muscle sheath, and occasionally significant expansion of the surrounding tunica adventitia, were noted even in a subset of macrocystic lesions with no identifiable systemic feeding vessel. Because the airways and arterial vascular supply of the normal lung (both the pulmonary arterial supply, as well as the normal bronchial arteries originating from the systemic circulation) are in close apposition and coordinately develop throughout lung branching morphogenesis, it is plausible that altered signaling from abnormal airway epithelium could lead to disordered arterial vascular growth, or even "recruit" an aberrant feeding vessel from the adjacent systemic circulation.

Despite the heterogeneity in histologic findings both within and across lesion types, and even within individual lesions, macrocystic CPAM lesions frequently showed distinct histopathologic characteristics including frequent abrupt

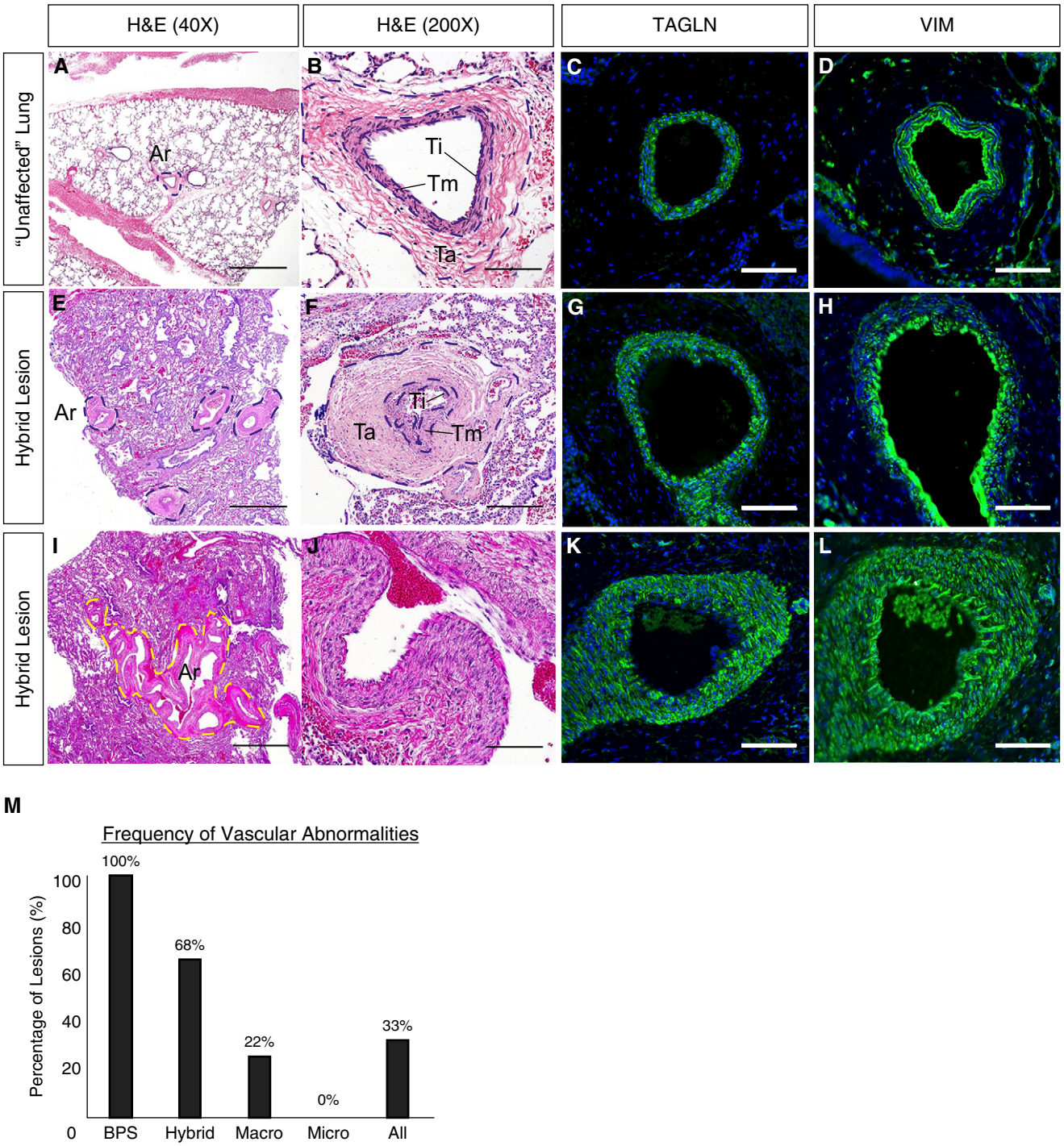

Figure 4. Abnormal arterial vascular development/remodeling in congenital lung lesions. In contrast to a healthy arteriole (*A–D*), hypertrophied and often tortuous arteries could be seen in nearly all BPS and hybrid lesions, as well as a subset of macrocystic lesions (*M*). (*E–L*) These arteries exhibited variable degrees of hypertrophy of the vascular smooth muscle ($TAGLN^+$), and outer layer (tunica adventitia) consisting of VIM^+ fibroblasts invested in a thick layer of extracellular matrix. Percentages in *M* refer to *N* = 58 patients. Ar = artery; BPS = bronchopulmonary sequestration; H&E = hematoxylin and eosin; Ta = tunica adventitia; TAGLN = transgelin; Ti = tunica intima; Tm = tunica media; VIM = vimentin. Scale bars: (*A*, *E*, and *I*) 500 μm; all others, 100 μm.

transitions in the larger cysts between relatively thick walls and alveolar-like sacs, minute papillary projections, and goblet cell metaplasia. Moreover, transcriptome data from all three lesion types suggest that whereas microcystic CPAM and hybrid lesions are related, macrocystic CPAM lesions may be transcriptionally distinct. Together, these data raise the question of whether these congenital lung lesions are in fact etiologically distinct or represent a spectrum of severity of the same disorder.

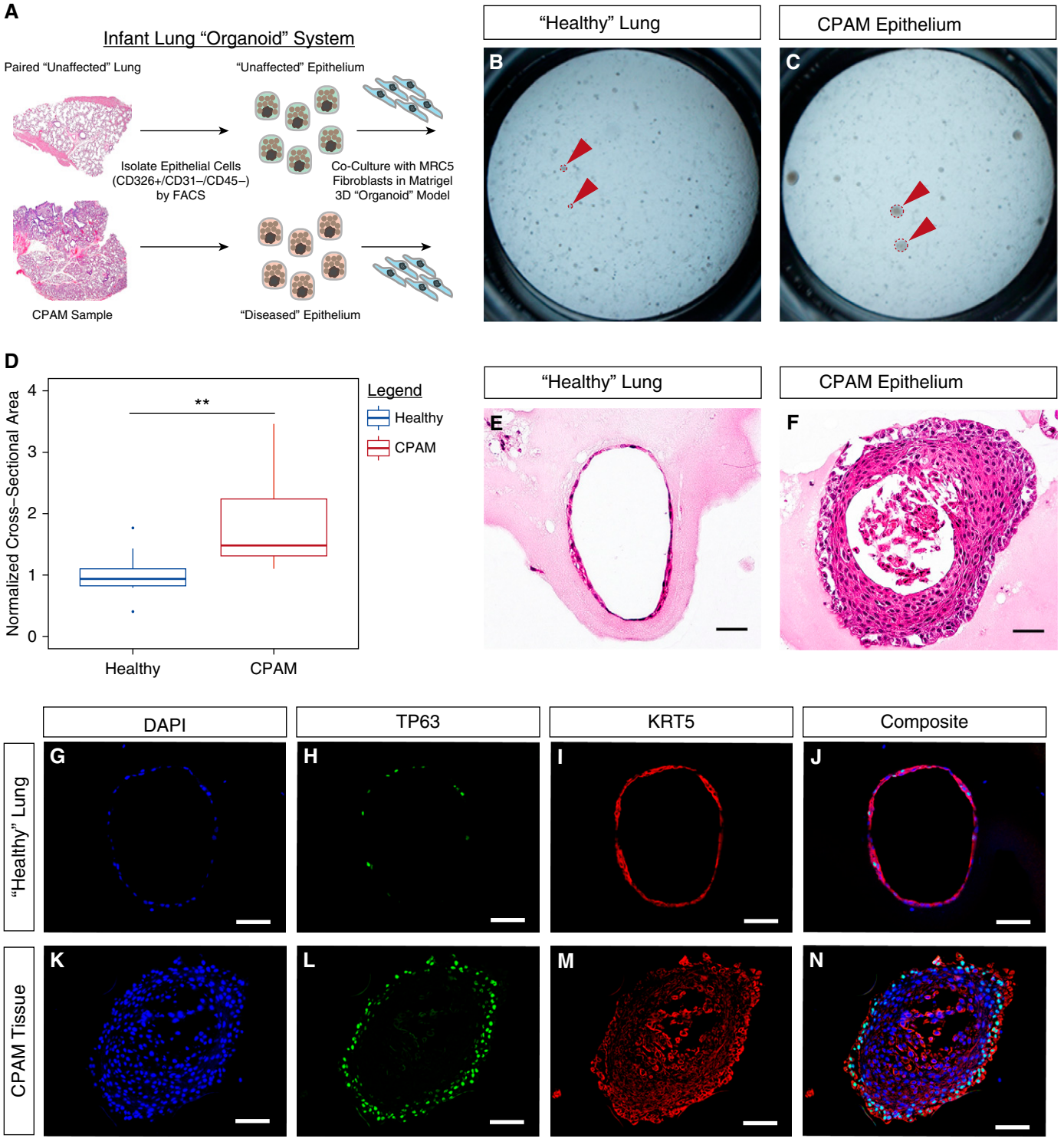

Figure 5. Epithelial cell-autonomous defects in congenital lung lesions. (*A*) A schematic illustration of the three-dimensional lung organoid culture system. (*B–F*) After 2 weeks in culture, the congenital pulmonary airway malformation (CPAM) epithelium formed larger organoids, as indicated by cross-sectional area (*D*), with thicker walls and smaller lumens (*B* and *C*, red arrowheads). (*E* and *G–J*) H&E and immunostaining demonstrate the presence of thin-walled spherelike organoids consisting of a single cell layer of predominantly $TP63^{+}/KRT5^{+}$ basal epithelium. (*F* and *K–N*) In contrast, epithelium isolated from the CPAM lesion formed dense spheres with thick walls of $TP63^{+}/KRT5^{+}$ basal cells at least two to three cell layers thick. FACS = fluorescence-activated cell sorting; H&E = hematoxylin and eosin; KRT5 = keratin, type II cytoskeletal 5; TP63 = tumor protein 63. $N = 3$ patients. Four technical replicates were performed per sample. Comparison of cross-sectional area with two-tailed Student's *t* test, $^{**}P < 0.01$. Scale bars, 50 μm.

We propose three general, but not mutually exclusive developmental etiologies for varying congenital lung malformations: *1*) each distinct category of lesion (macro, micro, hybrid, etc.) is etiologically distinct, with each lesion type originating from a distinct pathogenetic mechanism; *2*) the various categories of lesions originate from a related primary mechanism, but either the timing or anatomic location (e.g., proximal–distal location along the airway tree) imposes distinct characteristics on each lesion, similar to Stocker's proposal (2, 3); or *3*) lesions originate from related mechanisms occurring at similar times and locations during development, but quantitative differences in the molecular phenotype lead to a distinct morphologic category, for example, a modest reduction in PI3K–AKT–mTOR or Ras signaling leads to a small, asymptomatic microcystic CPAM lesion, whereas a larger reduction in the same signaling pathways leads to a large symptomatic macrocystic CPAM lesion with elements of goblet cell metaplasia.

The gene expression data set generated by this study provides the first comprehensive analysis of the transcriptional changes occurring within various types of congenital lung lesions. GSEA data highlight several molecular pathways that may play a role in the pathogenesis of this disorder, and provide targeted directions for future study. Downregulated transcripts were enriched in genes known to be positively regulated by *KRAS* signaling, and conversely upregulated transcripts were enriched for genes known to be negatively regulated by *KRAS* signaling, indicating a potential reduction of *KRAS* signaling in CPAM lesions. These observations are supported by mouse models where either activation or suppression of normal Ras/MAPK (mitogen-activated protein kinase) signaling can result in severe disruption of branching morphogenesis, in part through effects mediated by Sprouty-2 (32, 33). It also raises the possibility that activating *KRAS* G12D mutations, occasionally seen in a small number of cells in a subset of CPAM lesions, may occur because of ongoing cellular stress. Of note, this is the same oncogenic mutation seen in CPAM-associated and sporadic mucinous adenocarcinomas of the lung (34–37). GSEA demonstrated significant enrichment for members of the PI3K–AKT–mTOR signaling pathway among downregulated transcripts. PI3K–AKT signaling has been shown to regulate branching morphogenesis in mammary epithelium, also downstream of Sprouty-2, although this has not been studied in the murine lung *in vivo* (38). Somatic mutations in members of the PI3K–AKT–mTOR signaling pathway have been implicated in the pathogenesis of a wide array of structural birth defects, ranging from overgrowth syndromes to focal cortical dysplasia and vascular defects (39–41). However, only gain-of-function mutations have been reported to date. Finally, significant enrichment was observed for known Myc targets among the downregulated transcripts. N-myc has been shown in mice to play an essential role in proliferation and differentiation of the distal Sox9^{+} lung epithelial progenitor population, and overexpression of N-myc leads to an expansion of the distal lung epithelial compartment (42).

The *ex vivo* culture of epithelial cells isolated from CPAM lesions and paired adjacent "unaffected" lung provides support for a cell-autonomous defect in the epithelium of these lesions, which leads to disordered growth of proximal airway epithelial structures. This phenotype is present even after isolation from the diseased mesenchyme and when removed from complex mechanical and structural forces present *in vivo* that may impact the growth and differentiation of lung tissue (e.g., airway obstruction, mechanical compression). Together, these data suggest that a genetic or epigenetic defect in the lung epithelium plays a central role in the pathogenesis of at least a subset of congenital lung lesions.

We propose a model in which changes in the lung epithelium during branching morphogenesis lead to expansion of a disordered, irregular, and ectatic airway tree of varying severity, and that growth of this dysregulated airway epithelium disrupts the patterning of the closely associated arterial vasculature, occasionally leading to the recruitment of an aberrant systemic feeding

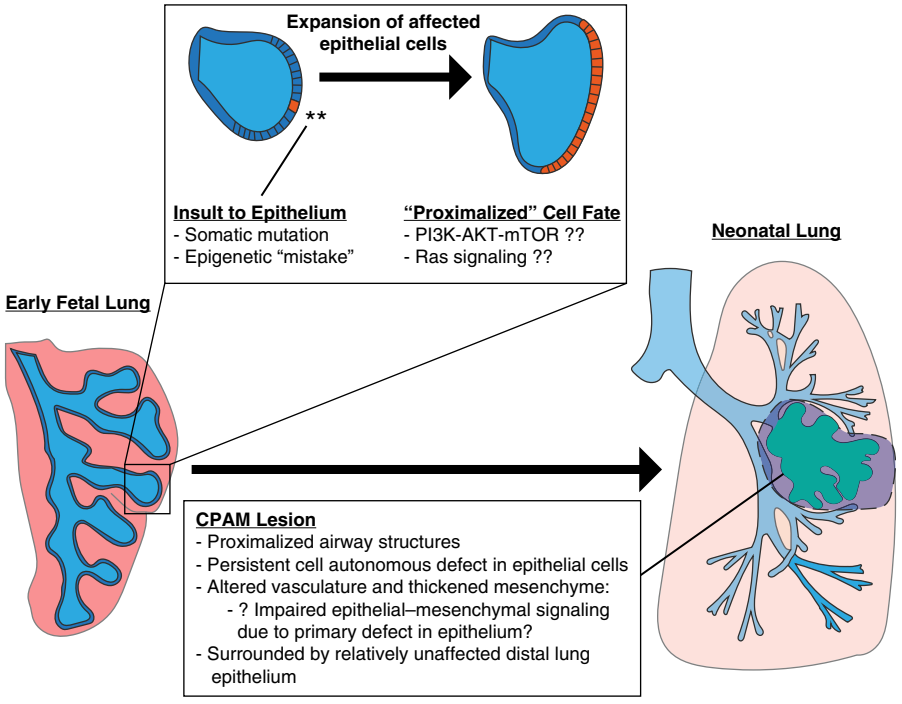

Figure 6. Proposed model diagram. We propose that a defect occurs during branching morphogenesis of the lung, such as a somatic mutation or alteration in chromatin state, that results in dysregulation of a key developmental signaling pathway such as Ras/MAPK or PI3K–AKT–mTOR signaling. This impaired epithelial population expands as development proceeds and remains "proximalized," forming an abnormal collection of cystic airway structures seen in the mature congenital lung lesion. Disrupted epithelial–mesenchymal interactions arising from these epithelial cells occasionally result in abnormal vascular development or may even "recruit" a systemic feeding vessel. CPAM = congenital pulmonary airway malformation; MAPK = mitogen-activated protein kinase; PI3K–AKT–mTOR = phosphatidylinositol 3-kinase–AKT–mammalian target of rapamycin.

vessel. In between these cystic airway structures, the distal lung tissue appears immature, with relatively large and simplified alveoli, and thickened interstitial spaces. It remains unclear whether these changes in the distal lung structures are simply the result of mechanical compression by the cystic regions leading to impaired alveolar development, or whether the same molecular insult resulting in expansion of the proximal airway structures also has a direct impact on distal lung development (43).

The developmental etiology of congenital lung lesions suggests that the initial molecular insult, such as a somatic mutation occurring during branching morphogenesis, could interact with other mechanisms including epigenetic, infectious, mechanical, or environmental exposures to instigate lesion development (Figure 6). Importantly, our gene expression data set highlights Ras and PI3K–AKT–mTOR signaling as candidate pathways warranting additional investigation. These data provide insight into the molecular and cellular basis of CPAM development and provide guidance for future studies. The study of congenital lung lesions provides unique insight into human lung development as well as other isolated structural birth defects and possible opportunities to explore pharmacologic modulation of disease for the most severely affected infants. ■

Author disclosures are available with the text of this article at www.atsjournals.org.

Acknowledgment: The authors thank Maria Fraga, M.D., Matthew Deardorff, M.D., and Ian Krantz, M.D., for support in the initial development of the Institutional Review Board protocol and subject consent.

References

1. Wilson RD, Hedrick HL, Liechty KW, Flake AW, Johnson MP, Bebbington M, *et al*. Cystic adenomatoid malformation of the lung: review of genetics, prenatal diagnosis, and *in utero* treatment. *Am J Med Genet A* 2006;140:151–155.
2. Stocker JT. Cystic lung disease in infants and children. *Fetal Pediatr Pathol* 2009;28:155–184.
3. Stocker JT, Madewell JE, Drake RM. Congenital cystic adenomatoid malformation of the lung: classification and morphologic spectrum. *Hum Pathol* 1977;8:155–171.
4. Laberge JM, Flageole H, Pugash D, Khalife S, Blair G, Filiatrault D, *et al*. Outcome of the prenatally diagnosed congenital cystic adenomatoid lung malformation: a Canadian experience. *Fetal Diagn Ther* 2001;16: 178–186.
5. Gornall AS, Budd JL, Draper ES, Konje JC, Kurinczuk JJ. Congenital cystic adenomatoid malformation: accuracy of prenatal diagnosis, prevalence and outcome in a general population. *Prenat Diagn* 2003; 23:997–1002.
6. Balayla J, Abenhaim HA. Incidence, predictors and outcomes of congenital diaphragmatic hernia: a population-based study of 32 million births in the United States. *J Matern Fetal Neonatal Med* 2014; 27:1438–1444.
7. Kapralik J, Wayne C, Chan E, Nasr A. Surgical versus conservative management of congenital pulmonary airway malformation in children: a systematic review and meta-analysis. *J Pediatr Surg* 2016;51: 508–512.
8. Tsai AY, Liechty KW, Hedrick HL, Bebbington M, Wilson RD, Johnson MP, *et al*. Outcomes after postnatal resection of prenatally diagnosed asymptomatic cystic lung lesions. *J Pediatr Surg* 2008;43:513–517.
9. Bush A. Congenital lung disease: a plea for clear thinking and clear nomenclature. *Pediatr Pulmonol* 2001;32:328–337.
10. Clements BS, Warner JO. Pulmonary sequestration and related congenital bronchopulmonary–vascular malformations: nomenclature and classification based on anatomical and embryological considerations. *Thorax* 1987;42:401–408.
11. Langston C. New concepts in the pathology of congenital lung malformations. *Semin Pediatr Surg* 2003;12:17–37.
12. Adzick NS, Harrison MR, Glick PL, Golbus MS, Anderson RL, Mahony BS, *et al*. Fetal cystic adenomatoid malformation: prenatal diagnosis and natural history. *J Pediatr Surg* 1985;20:483–488.
13. Gonzaga S, Henriques-Coelho T, Davey M, Zoltick PW, Leite-Moreira AF, Correia-Pinto J, *et al*. Cystic adenomatoid malformations are induced by localized FGF10 overexpression in fetal rat lung. *Am J Respir Cell Mol Biol* 2008;39:346–355.
14. Nyeng P, Norgaard GA, Kobberup S, Jensen J. FGF10 maintains distal lung bud epithelium and excessive signaling leads to progenitor state arrest, distalization, and goblet cell metaplasia. *BMC Dev Biol* 2008;8:2.
15. Cardoso WV, Itoh A, Nogawa H, Mason I, Brody JS. FGF-1 and FGF-7 induce distinct patterns of growth and differentiation in embryonic lung epithelium. *Dev Dyn* 1997;208:398–405.
16. Shiratori M, Oshika E, Ung LP, Singh G, Shinozuka H, Warburton D, *et al*. Keratinocyte growth factor and embryonic rat lung morphogenesis. *Am J Respir Cell Mol Biol* 1996;15:328–338.
17. Jancelewicz T, Nobuhara K, Hawgood S. Laser microdissection allows detection of abnormal gene expression in cystic adenomatoid malformation of the lung. *J Pediatr Surg* 2008;43:1044–1051.
18. Cass DL, Quinn TM, Yang EY, Liechty KW, Crombleholme TM, Flake AW, Adzick NS. Increased cell proliferation and decreased apoptosis characterize congenital cystic adenomatoid malformation of the lung. *J Pediatr Surg* 1998;33:1043–1046; discussion 1047.
19. Volpe MV, Chung E, Ulm JP, Gilchrist BF, Ralston S, Wang KT, *et al*. Aberrant cell adhesion molecule expression in human bronchopulmonary sequestration and congenital cystic adenomatoid malformation. *Am J Physiol Lung Cell Mol Physiol* 2009;297: L143–L152.
20. Weber SC, Sallmon H, Sarioglu N, Degenhardt P, Bührer C, Rüdiger M, *et al*. The expression of vascular endothelial growth factor and its receptors in congenital bronchopulmonary cystic malformations. *Eur J Pediatr Surg* 2012;22:127–132.
21. Lantuejoul S, Nicholson AG, Sartori G, Piolat C, Danel C, Brabencova E, *et al*. Mucinous cells in type 1 pulmonary congenital cystic adenomatoid malformation as mucinous bronchioloalveolar carcinoma precursors. *Am J Surg Pathol* 2007;31:961–969.
22. Kunisaki SM, Fauza DO, Nemes LP, Barnewolt CE, Estroff JA, Kozakewich HP, *et al*. Bronchial atresia: the hidden pathology within a spectrum of prenatally diagnosed lung masses. *J Pediatr Surg* 2006;41:61–65; discussion 61–65.
23. Riedlinger WF, Vargas SO, Jennings RW, Estroff JA, Barnewolt CE, Lillehei CW, *et al*. Bronchial atresia is common to extralobar sequestration, intralobar sequestration, congenital cystic adenomatoid malformation, and lobar emphysema. *Pediatr Dev Pathol* 2006;9: 361–373.
24. Herriges MJ, Swarr DT, Morley MP, Rathi KS, Peng T, Stewart KM, *et al*. Long noncoding RNAs are spatially correlated with transcription factors and regulate lung development. *Genes Dev* 2014;28:1363–1379.
25. Frank DB, Peng T, Zepp JA, Snitow M, Vincent TL, Penkala IJ, *et al*. Emergence of a wave of Wnt signaling that regulates lung alveologenesis by controlling epithelial self-renewal and differentiation. *Cell Reports* 2016;17:2312–2325.
26. Davenport M, Warne SA, Cacciaguerra S, Patel S, Greenough A, Nicolaides K. Current outcome of antenally diagnosed cystic lung disease. *J Pediatr Surg* 2004;39:549–556.
27. Pogoriler J, Swarr D, Kreiger P, Adzick NS, Peranteau W. Congenital cystic lung lesions: redefining the natural distribution of subtypes and assessing the risk of malignancy. *Am J Surg Pathol* [online ahead of print] 20 Dec 2017; DOI: 10.1097/PAS.0000000000000992.
28. Flecknoe SJ, Wallace MJ, Cock ML, Harding R, Hooper SB. Changes in alveolar epithelial cell proportions during fetal and postnatal development in sheep. *Am J Physiol Lung Cell Mol Physiol* 2003;285:L664–L670.
29. Rock JR, Onaitis MW, Rawlins EL, Lu Y, Clark CP, Xue Y, *et al*. Basal cells as stem cells of the mouse trachea and human airway epithelium. *Proc Natl Acad Sci USA* 2009;106:12771–12775.

30. Stoerke O. Ueber angeborene blasige Missbildung der Lunge. *Wien Klin Wochenschr* 1897;2:25–31.
31. Kunisaki SM, Ehrenberg-Buchner S, Dillman JR, Smith EA, Mychaliska GB, Treadwell MC. Vanishing fetal lung malformations: prenatal sonographic characteristics and postnatal outcomes. *J Pediatr Surg* 2015;50:978–982.
32. Guerra C, Mijimolle N, Dhawahir A, Dubus P, Barradas M, Serrano M, *et al*. Tumor induction by an endogenous K-ras oncogene is highly dependent on cellular context. *Cancer Cell* 2003;4:111–120.
33. Shaw AT, Meissner A, Dowdle JA, Crowley D, Magendantz M, Ouyang C, *et al*. Sprouty-2 regulates oncogenic K-ras in lung development and tumorigenesis. *Genes Dev* 2007;21:694–707.
34. Kadota K, Yeh YC, D'Angelo SP, Moreira AL, Kuk D, Sima CS, *et al*. Associations between mutations and histologic patterns of mucin in lung adenocarcinoma: invasive mucinous pattern and extracellular mucin are associated with KRAS mutation. *Am J Surg Pathol* 2014; 38:1118–1127.
35. Ishida M, Igarashi T, Teramoto K, Hanaoka J, Iwai M, Yoshida K, *et al*. Mucinous bronchioloalveolar carcinoma with K-ras mutation arising in type 1 congenital cystic adenomatoid malformation: a case report with review of the literature. *Int J Clin Exp Pathol* 2013;6:2597–2602.
36. Singh G, Coffey A, Neely R, Lambert D, Sonett J, Borczuk AC, *et al*. Pulmonary Kirsten rat sarcoma virus mutation positive mucinous adenocarcinoma arising in a congenital pulmonary airway malformation, mixed type 1 and 2. *Ann Thorac Surg* 2016;102: e335–e337.
37. Summers RJ, Shehata BM, Bleacher JC, Stockwell C, Rapkin L. Mucinous adenocarcinoma of the lung in association with congenital pulmonary airway malformation. *J Pediatr Surg* 2010;45:2256–2259.
38. Zhu W, Nelson CM. PI3K regulates branch initiation and extension of cultured mammary epithelia via Akt and Rac1 respectively. *Dev Biol* 2013;379:235–245.
39. Lim KC, Crino PB. Focal malformations of cortical development: new vistas for molecular pathogenesis. *Neuroscience* 2013;252:262–276.
40. Limaye N, Kangas J, Mendola A, Godfraind C, Schlögel MJ, Helaers R, *et al*. Somatic activating PIK3CA mutations cause venous malformation. *Am J Hum Genet* 2015;97:914–921.
41. Lindhurst MJ, Parker VE, Payne F, Sapp JC, Rudge S, Harris J, *et al*. Mosaic overgrowth with fibroadipose hyperplasia is caused by somatic activating mutations in PIK3CA. *Nat Genet* 2012;44:928–933.
42. Okubo T, Knoepfler PS, Eisenman RN, Hogan BL. Nmyc plays an essential role during lung development as a dosage-sensitive regulator of progenitor cell proliferation and differentiation. *Development* 2005;132:1363–1374.
43. Moessinger AC, Harding R, Adamson TM, Singh M, Kiu GT. Role of lung fluid volume in growth and maturation of the fetal sheep lung. *J Clin Invest* 1990;86:1270–1277.